A Computer Code for Calculating Tropospheric and Ionospheric Refraction Effects on Radar Systems

Robert E. Daniell, Jr.
Independent Consultant
38 Sandy Ridge Road
Stoughton, MA 02072-2226
(781) 344-6966
daniell@ionosphericphysics.com

Charles S. Carrano, Gina M. Gugliotti Fishman, and Nelson A. Bonito
Atmospheric and Environmental Research, Inc., USA

***Abstract*— We have developed the Tropospheric and Ionospheric Radar Refraction (TIRR) code which calculates refraction effects by performing two-dimensional ray tracing through tropospheric and ionospheric specification models. We have performed preliminary tests using the output from a tropospheric model and an ionospheric model that each assimilate actual data to provide near real-time global specifications of their respective atmospheric regions. We present the results of three such runs for the radar system located at Eglin AFB: (1) a baseline run, (2) a run for a nearby hurricane, and (3) a run for a severely disturbed ionosphere. Generally, we find that range error is dominated by the ionosphere, except at low elevation angles where tropospheric refraction becomes more important. We also discuss plans for more extensive tests as well as for augmentation of the model to allow for airborne radar systems and three-dimensional ray tracing.**

I. Introduction

As target tracking requirements have become more demanding, the need for accurate calculation and prediction of atmospheric refraction effects on radar systems has become more important. To meet this need we are developing a Tropospheric and Ionospheric Radar Refraction (TIRR) Code for use with gridded atmospheric (ionospheric and tropospheric) specifications and forecasts. The atmospheric specifications can be based on data assimilation specification and forecast models as well as on climatological models so that TIRR can be used in real-time applications and forecasts as well as in design and performance studies. The output of the atmospheric specifications must be in the form of electron density for the ionosphere and pressure, temperature, and water vapor pressure for the troposphere, and must be produced on a regular grid of latitude, longitude, and altitude that at least covers the region visible to the radar. Global specifications and models are preferred because they permit calculations for multiple radar sites.

TIRR converts the atmospheric specification from its native latitude-longitude-altitude grid to a three-dimensional azimuth-elevation-range grid (the "radar grid") centered on the radar site. TIRR then performs a two-dimensional ray trace through the radar grid, calculating the index of refraction as it goes. (For the bulk ionosphere, the vertical gradients are much larger than the horizontal gradients, so azimuthal refraction is neglected.) The two-dimensional ray tracing algorithm is based on a method developed by G. H. Millman [1] and was implemented in the Ionospheric Error Correction Model (IECM) that is in operational use by the ALTAIR system at the Kwajalein Missile Range [2]. It is a forward algorithm that traces a ray with an *apparent* azimuth and elevation as it propagates through the atmosphere to determine the *true* elevation and range along the ray path.

The output of TIRR includes range error and elevation error and, if the radar frequency bandwidth is provided, pulse dispersion. The output is provided on a three-dimensional grid of apparent azimuth, elevation, and range. The atmospheric corrections for range and elevation error for single or multiple targets can be easily obtained by interpolation in the output grid. Note that although the initial version of TIRR assumes a transmitter located at the surface of the Earth, this condition will be relaxed in future versions allowing for airborne and space based transmitters.

II. Preliminary Test Results

In this paper we show the results of initial tests of TIRR using tropospheric and ionospheric specifications based on real data from four periods during 2005-2006. We have selected the AN/FPS85 Spacetrack Radar system located at Eglin AFB as the example for the TIRR runs. The four dates and times and the atmospheric and ionospheric conditions for which we have TIRR output are indicated in Table I.

The tropospheric specifications were supplied by the National Center for Environmental Prediction (NCEP), using the Global Forecast System (GFS) driven by environmental measurements from the Global Data Assimilation System (GDAS). The ionospheric specifications were supplied by the C/NOFS Data Center at Hanscom AFB, using the Utah State University (USU) Ionospheric Forecast Model (IFM) driven by GPS measurements from the Crustal Dynamics Data Information System (CDDIS). The TIRR calculations were performed assuming a radar operating frequency of 442 MHz for all cases presented here.

The baseline case (January 17, 2006), for which both the troposphere and ionosphere were relatively undisturbed over Eglin AFB, is illustrated in Fig. 1. The results of the TIRR run for this case are shown in Figs. 2-4. Fig. 2 shows the range and elevation errors as a function of range at an

TABLE I
CONDITIONS FOR THE FOUR CASES THAT HAVE BEEN ANALYZED SO FAR

Date	Time (UT)	Time (Local)	Tropospheric conditions at Eglin AFB	Ionospheric conditions at Eglin AFB
January 21, 2005 (day 21)	2300	1712	Undisturbed	Storm enhanced density, strong gradient toward WNW
June 10, 2005 (day 161)	1200	0612	Hurricane Arlene	Undisturbed, dawn density gradient
August 29, 2005 (day 241)	1200	0612	Hurricane Katrina	Undisturbed, dawn density gradient
January 17, 2006 (day 17)	0000	1812	Baseline (undisturbed)	Baseline (undisturbed, early evening)

apparent elevation of 1°. Note that while the troposphere is non-dispersive, the ionospheric refraction is frequency dependent. In order to estimate the relative importance of the troposphere and the ionosphere, we estimated the ionospheric range error from

$$R_{iono} = \frac{40.3 \times \mathrm{TEC}}{f^2} \quad (1)$$

and subtracted this from the total range error to obtain the tropospheric contribution. These are shown in Fig. 3, again for an elevation of 1°. The ratio of the ionospheric contribution to the tropospheric contribution at elevations of 1° and 10° are shown in Fig. 4. Although the troposphere is important at very low elevations, above 10° the ionosphere dominates, at least in this case.

Due to space limitations, we will discuss only one of the hurricane cases, namely Hurricane Katrina (August 29, 2005), simply because it had the largest water vapor content over Eglin at the chosen time. The ionospheric and tropospheric conditions are shown in Fig. 5 and the results of the TIRR run are shown in Figs. 6-8.

A disturbed ionosphere case is shown in Figs. 9-12. The troposphere is relatively undisturbed but there is a large (geomagnetic) storm enhanced electron density over the western United States causing a large density gradient over Eglin. The enhanced electron density causes the ionosphere to dominate the range error in westward directions even at low elevation angles.

III. PLANS FOR THE FUTURE

In order to rigorously test the model, we would like to identify a case where we have good specification of the troposphere and the ionosphere as well as radar measurements of calibration objects so that we can determine the actual range and elevation errors with some precision.

Once the TIRR code has been thoroughly tested, there are several enhancements we plan to introduce. The first and easiest is to generalize the code to allow for airborne radar systems. The second enhancement is to introduce 3D ray tracing so that the code can accommodate models that include small scale structures and inhomogeneities in the ionosphere. These structures include the low latitude ionospheric "bubbles," polar cap patches, and various kinds of auroral arcs. The low latitude bubbles form shortly after sunset and lead to Equatorial Spread F (ESF) as well as scintillation on transionospheric communications signals. Polar cap patches are formed by the transport of high density daytime plasma into the nightside high latitude ionosphere. Auroral arcs form not only in the auroral region but in the polar cap in response to transient electron and ion precipitation events. Among the three-dimensional ray tracing algorithms being considered is the Jones-Stephenson algorithm [3], which is available from NOAA, and is widely used.

ACKNOWLEDGMENT

This work was sponsored by Air Force Contract FA8718-06-C-0035 with Atmospheric and Environmental Research, Inc. The IFM model was developed by the IFM team (R.W. Schunk, L. Scherliess, J.J. Sojka, D.C. Thompson, and L. Zhu) at Utah State University.

REFERENCES

[1] G. H. Millman, Atmospheric effects in VHF and UHF propagation, *Proceedings of the IRE*, vol. 46, pp. 1492-1501, August 1958.

[2] S. M. Hunt, S. Close, A. J. Coster, E. Stevens, L. M. Schuett, and A. Vardaro, Equatorial Atmospheric and Ionospheric Modeling at Kwajalein Missile Range, *Lincoln Laboratory Journal*, vol. 12, no. 1, pp. 45-64, 2000

[3] R. M. Jones and J. J. Stephenson, A versatile three-dimensional ray tracing computer program for radio waves in the ionosphere. OT Report 75-76. PB2488567, 1975.

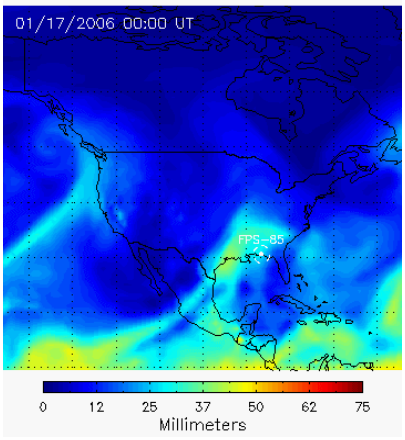

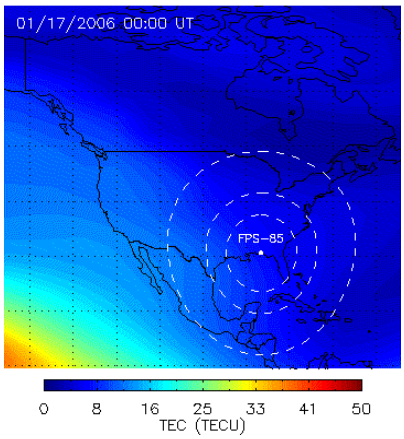

Fig. 1. Precipitable water vapor (mm) for the troposphere (left panel) and vertical TEC (TEC units or TECU) for the ionosphere (right panel) for the baseline case (January 17, 2006). The location of the FPS-85 radar at Eglin AFB is indicated along with level curves of 0°, 10°, and 20° elevation projected onto the altitudes 2.5 km (left panel) and 350 km (right panel) (the approximate centroid heights of water vapor density and electron density, respectively). Both the troposphere and the ionosphere are relatively undisturbed. (1 TECU = 10^{16} electrons m^{-2}.)

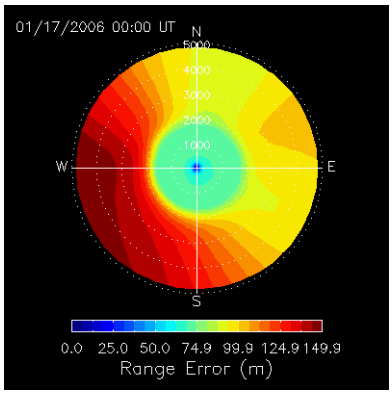

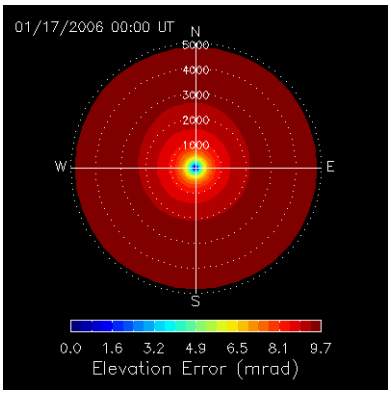

Fig. 2. Range error (m, left panel) and elevation error (mrad, right panel) for an elevation of 1° for the baseline case of Fig. 1. The dashed circles indicate the range from 0 to 5000 km in steps of 1000 km.

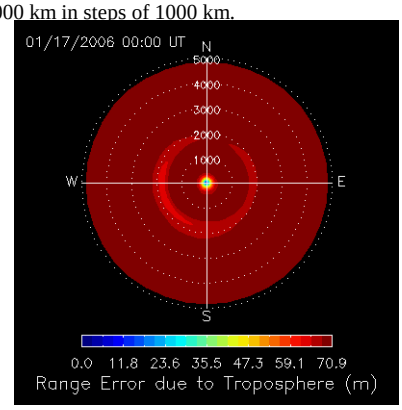

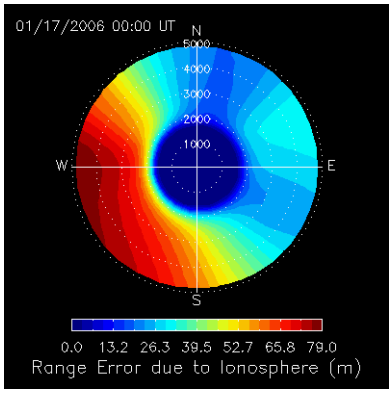

Fig. 3. An estimate of the separate contributions to range error of the troposphere (left panel) and the ionosphere (right panel) at an elevation of 1°.

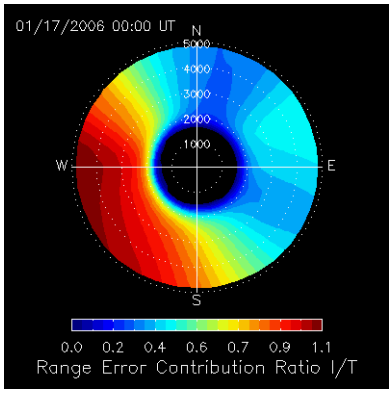

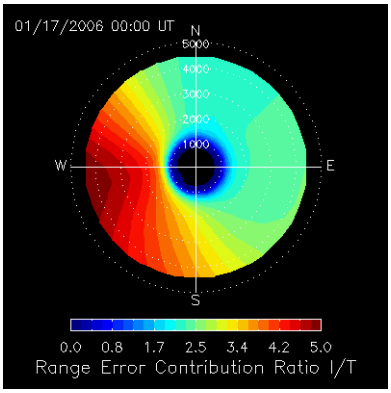

Fig. 4. The ratio of the ionospheric to tropospheric contributions to range error at 1° elevation (left panel) and at 10° elevation (right panel). Above 10° elevation the ionosphere dominates the range error except at very small ranges (when the target is below the ionosphere).

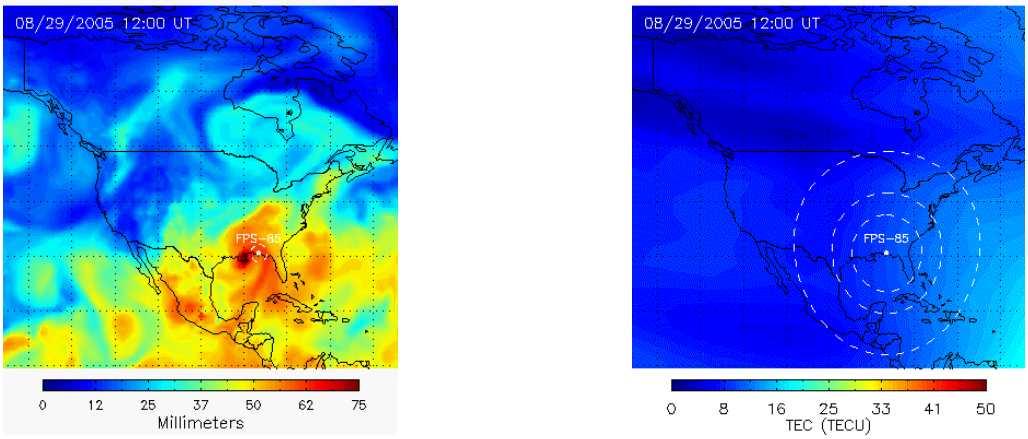

Fig. 5. Precipitable water vapor (mm) for the troposphere (left panel) and vertical TEC (TECU) for the ionosphere (right panel) for the disturbed troposphere case (Hurricane Katrina, August 29, 2005). The ionosphere is relatively undisturbed although there is a density gradient toward the east due to sunrise. The water vapor densities, on the other hand, are quite high over Eglin even though the hurricane is well to the west at this time.

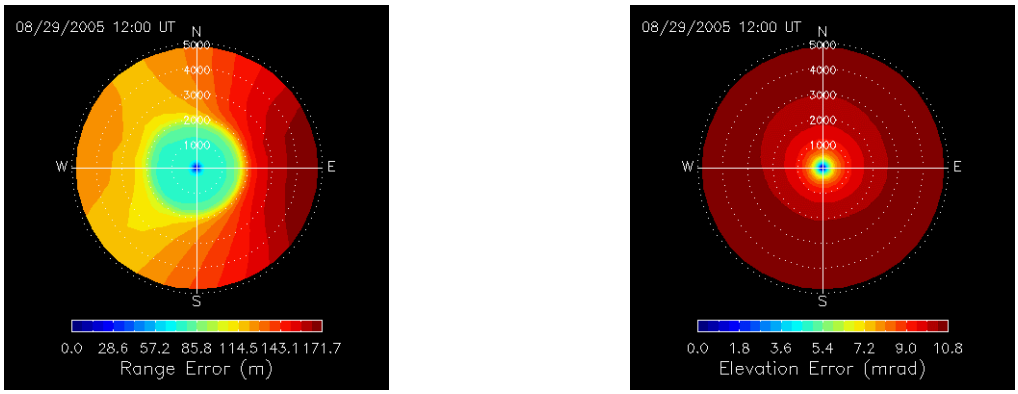

Fig. 6. Range error (m, left panel) and elevation error (mrad, right panel) for an elevation of 1° for the disturbed troposphere case of Fig. 5. The dashed circles indicate the range from 0 to 5000 km in steps of 1000 km.

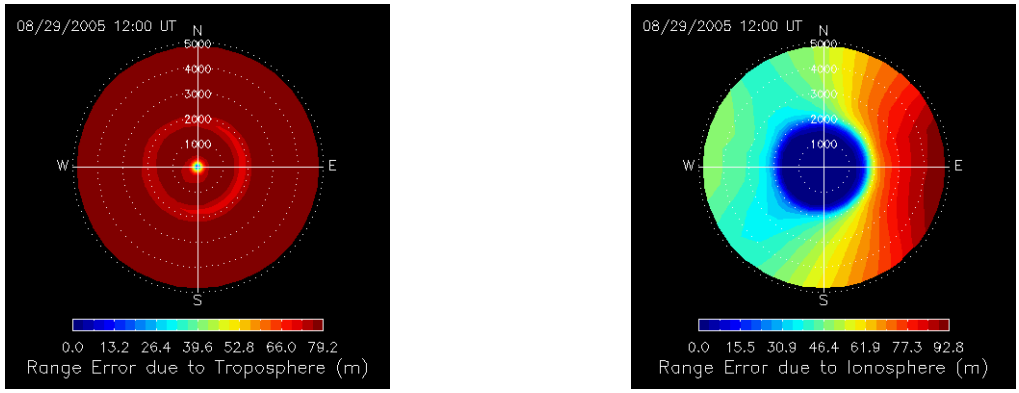

Fig. 7. An estimate of the separate contributions to range error of the troposphere (left panel) and the ionosphere (right panel) at an elevation of 1°.

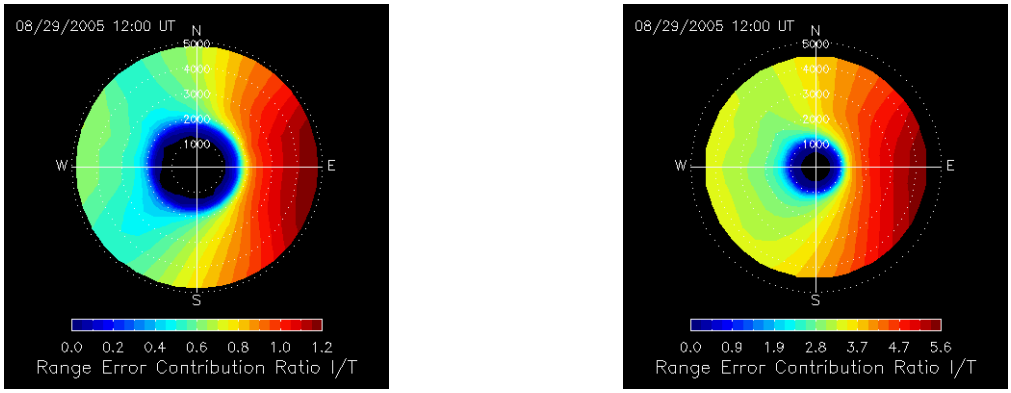

Fig. 8. The ratio of the ionospheric to tropospheric contributions to range error at 1° elevation (left panel) and at 10° elevation (right panel). Above 10° elevation the ionosphere dominates the range error except at very small ranges (when the target is below the ionosphere).

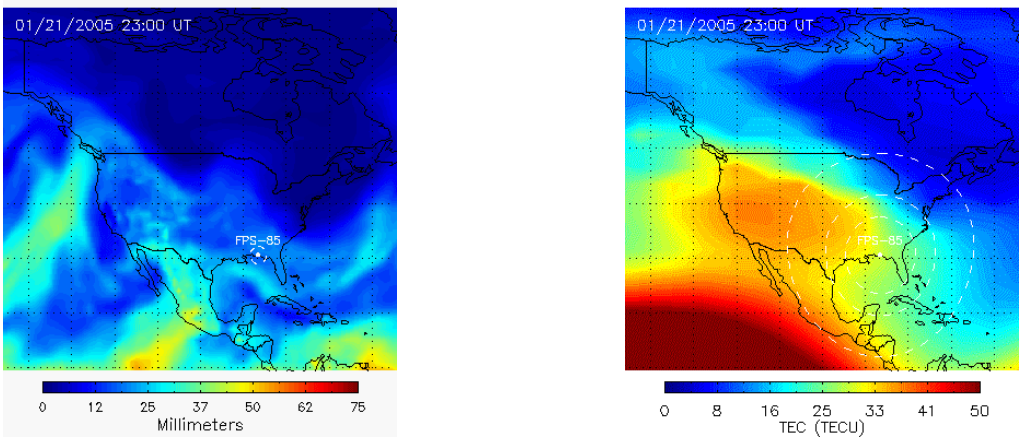

Fig. 9. Precipitable water vapor (mm) for the troposphere (left panel) and vertical TEC (TECU) for the ionosphere (right panel) for the disturbed ionosphere case (January 21, 2005). The troposphere is relatively undisturbed with relatively low water vapor densities over Eglin. Although the storm enhanced TEC is located over the western United States, there is a strong east-west gradient over Eglin.

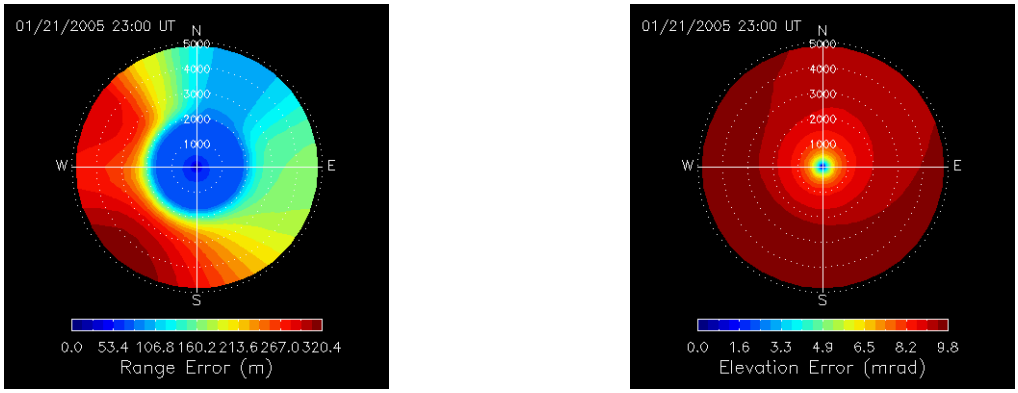

Fig. 10. Range error (m, left panel) and elevation error (mrad, right panel) for an elevation of 1° for the disturbed ionosphere case of Fig. 9. The dashed circles indicate the range from 0 to 5000 km in steps of 1000 km.

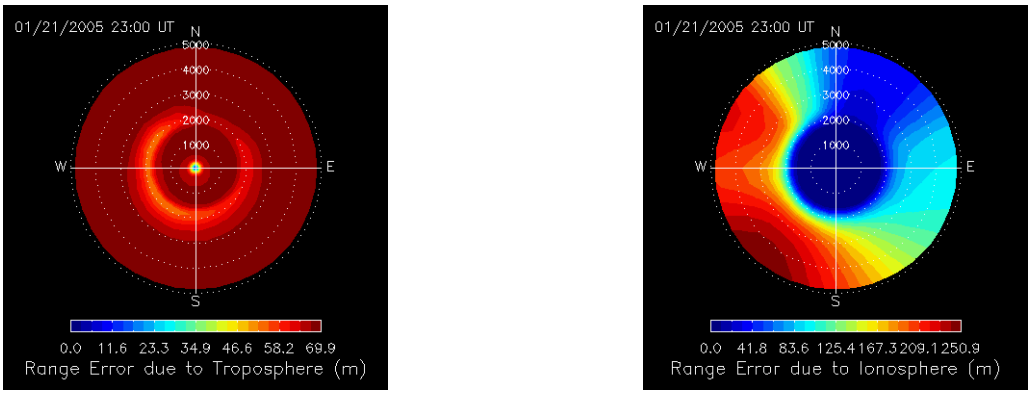

Fig. 11. An estimate of the separate contributions to range error of the troposphere (left panel) and the ionosphere (right panel) at an elevation of 1°.

Fig. 12. The ratio of the ionospheric to tropospheric contributions to range error at 1° elevation (left panel) and at 10° elevation (right panel). Due to the storm enhanced densities to the west of Eglin, the ionosphere dominates the range error even at 1° elevation in westward azimuths.